A FRACTURE MECHANICS BASED DESCRIPTION OF THE PROPAGATION BEHAVIOUR OF SMALL CRACKS AT NOTCHES

J. FOTH*, R. MARISSEN**, H. NOWACK**, G. LÜTJERING***

The nucleation and propagation behaviour of small cracks in the technical Al-2024-T3 alloy was investigated. Microstructural influences as inclusions which are present from the manufacturing process were found to be important for the crack initiation process. The propagation of the small cracks could be described using a J-integral based stress intensity factor(in order to account for the elastic-plastic deformations)together with an Elber type crack propagation equation.

It was found that the small cracks behaved in a similar manner as long cracks.

INTRODUCTION

A large part of the fatigue life of engineering structures or components is covered by the initiation and the growth of small cracks. That is the reason why an increasing number of investigations considers this part of the fatigue life [1,2]. In the literature numerous differences between the behaviour of small cracks as compared to long cracks have been observed (e.g. [3]). In the case of notches so-called non-propagating cracks were found. In other cases the growth rates of small cracks appeared to be much greater than those for long cracks. Even at stress intensities below ΔK_{th} crack growth was found.

Since most engineering components exhibit notches, the stress gradients and - in the case of elastic-plastic deformations at the notch - the local plasticity has to be taken into account. Modern crack initiation life prediction methods as the numerical notch analysis often give quite accurate results of the crack initiation life [4,5]. The prediction capability of the methods increases, the smaller the initial crack length for the end of the crack initiation stage is chosen. On the other side the inaccuracy of crack propagation analyses increases the more the crack length approaches microstructural sizes. A main cause is that at the short crack lengths microstructural parameters, as grain size, inclusion content, weak zones etc. dominate the crack growth behaviour and that they are not taken into account in the long crack prediction methods. This is the reason why new prediction methods on the basis of fracture mechanics for the growth behaviour of small

* IABG, D 8012 Ottobrunn, formerly DFVLR, Institut für Werkstoff-Forschung, D 5000 Köln 90, W.-Germany
** DFVLR, Institut für Werkstoff-Forschung, D 5000 Köln 90, W.-Germany
*** Technische Universität Hamburg-Harburg, D 2100 Hamburg-Harburg,W.-Germany

cracks have to be developed. Plasticity, stress gradients and the microstructure of the material are important influencing factors. Some possibilities to allow for these influencing factors are outlined in the following sections.

EXPERIMENTAL PROGRAM

For the evaluation of the crack initiation life and of the propagation behaviour of small cracks the following fatigue tests were performed on double edge notched (K_t = 1.22 and K_t = 3.3) and unnotched (K_t = 1.0) specimens (which were taken from flat sheets of a thickness of 4.7 mm). The Al-2024-T3 material as used in this study contained small amounts of Fe and Si from the manufacturing process. These elements form coarse intermetallic inclusions with the alloying elements.

In order to be able to compare the crack initiation and small crack behaviour of the notched and unnotched specimens a same local strain history was applied at the notch root of the notched specimens and at the surface of the unnotched specimens. This is in general accordance with the companion specimen concept which was originally proposed by Crews and Hardrath [6].

The fatigue tests were done in closed-loop servohydraulic machines, once at constant strain amplitudes of ε = 0.7±0.3 % and of ε = 0.85±0.15 % and once with simple variable amplitude loading (block loading), which represented combinations of the two constant amplitude histories.

The initiation of cracks and the crack propagation was observed by means of light microscopes (compare [1]). After the tests microstructural investigations were performed including scanning electron microscope fractography.

RESULTS AND DISCUSSION

Crack initiation

The crack nucleation in the fatigue experiments is dominated by the applied loads as well as by microstructural phenomena. On a microscopic scale plastic deformations occur especially due to the motion of dislocations. Materials which show an inhomogeneous slip deformation tend to an early crack nucleation because of the concentrated pile-up of dislocations. In Fig. 1 an overview of the influence of various microstructural parameters on the crack nucleation and on the crack propagation behaviour under static and cyclic loading is given [7]. As already mentioned, the material as it is considered here contained intermetallic inclusions. The size was 1 - 10 µm. The inclusions act as stress concentrations which lead to strongly localized plastic deformations even at low stress levels. Because of the brittle nature of the inclusions they cannot deform like the surrounding matrix material. That leads to the failure of these inclusions during the fatigue loading. From the cracked inclusions microcracks start to propagate into the matrix material (compare Figs. 2,3). At first the individual microcracks grow independently of each other until they reach a certain size. If the stress fields of the microcracks start to interact, some of the cracks begin to coalesce and form the basis of the later macrocrack. The individual stages of the described processes are given in more detail in [1].

For the evaluation of the influence of stress raisers at notches it is worthwhile to investigate the fatigue behaviour of unnotched specimens first, and to compare the observed behaviour to that of the notched specimens. According to the already mentioned companion specimen concept by Crews and

Hardrath it was assumed that the notched specimen exhibited an equivalent crack initiation behaviour as unnotched specimens, if the same strain history is applied in both cases (compare Fig. 4). Fig. 5 shows the results of the tests which were performed in this study. It can be seen that the assumed equivalence is observed at high strain levels only. As the strain level is decreased and approaches the endurance limit of the material, considerable differences between the notched and the unnotched specimen behaviour are observed. The unnotched specimens show the shortest fatigue life. This is mainly due to the following reasons: At the notched specimens the stresses and strains decrease with an increasing distance from the notch root surface. Because of the microsupport effect due to the less severely loaded grains below the highly loaded surface grains the probability for the initiation of cracks is higher for the unnotched specimens than for the notched specimens. Secondly, because of the larger surface area with high strains in the case of the unnotched specimens the probability of the initiation of cracks is again higher (statistical size effect).

In Fig. 6 the sum of the individual lengths of those surface cracks which later form the macrocrack is plotted versus the number of cycles for the three different types of specimens. Crack initiation was defined as that number of cycles at which those inclusions were broken, where the later dominating macrocrack started from. Under the constant amplitude loading with local strains of ε = 0.7±0.3 % the cycle number to crack initiation was nearly the same for all three types of the specimens. With increasing crack length larger differences in the crack growth behaviour for the different types of specimens are observed. The unnotched specimens with the homogeneous (high) net section stress show the highest growth rates and the earliest failure. Due to the decreasing stress fields the notched specimens fail significantly later.

From the described observations it can be concluded that the equivalence concept is mainly valid for the crack initiation life behaviour in the limited life range only. It looses its significance the longer the crack length which terminates the crack initiation stage is chosen. If the complete fracture of the specimen is taken as the failure criterion, the equivalence concept is not valid. These results are important for the application of the notch root concepts to engineering problems. The situation becomes more complex in the case of variable amplitude loading where additionally load sequence effects occur. These problems are treated in more detail in [8].

Crack propagation

The considerations as they were presented in the preceding section can only give a global view of the microcrack propagation behaviour. In [1] a procedure has been proposed for the evaluation of the stress intensity factor for semielliptical surface cracks at notches. In Fig. 7 an improved superposition concept for the stress intensity is given. By means of this concept the stress gradient along the entire crack front of the semielliptical surface crack can be considered. The concept represents a similarity consideration: The influence of the stress gradient for the semielliptical surface cracks (as expressed by the ratio K_{NEC}/K_{EC}) is assumed to be similar as the influence of the stress gradient in embedded cracks (as expressed by the ratio K_{NCC}/K_{CC}). (The stress gradient at both sides of the embedded cracks is chosen to be the same as for the considered cracks in a notch.) The exact solutions for the two stress intensity factors, K_{NCC} and K_{CC}, can be taken from the literature. The stress gradient has to be considered by the use of a polynominal equation which may be derived from FEM-calculations of the stress-strain distribution of the notched specimen [10].

The stress intensity factor for a semielliptical surface crack for the unnotched specimen K_{EC} can be calculated using Newman's approximate solution [11]. The described similarity approach gives the solution for the stress intensity factor of a semielliptical surface crack within a notch stress field K_{NEC} and is valid along the entire crack front. For the calculation of K_{NEC} (compare Fig. 8) certain amounts of a and c (with a as the crack depth and c as the half surface crack length) have to be chosen. The amounts of the stress intensity factors at point A and B (compare Fig. 8) can then be calculated. The crack growth increments according to the stress intensity factors at point A and B, respectively, were derived from the basic da/dN-ΔK data of the material. These crack growth increments were added to the amount of the instantaneous crack lengths a and c, respectively. If calculations of this type are performed in a cycle by cycle manner, they always lead to a stabilized shape of the semielliptical surface cracks with an aspect ratio of a/c = 0.9, which is in very close agreement to the experimentally observed crack shapes.

Using this calculation method the differences in the stress intensity factors could be determined for the three types of specimens. They are given in Fig. 9. The results in Fig. 9 clearly show that the increase in the crack growth rates for the notched specimens is significantly smaller than for the unnotched specimens as the crack length increases (due to the influence of the stress gradient (compare Fig. 6)).

Until now calculations of the microcrack growth rates using long crack data as a basis were only possible as long as plasticity effects were neglected. In order to allow for the plasticity effects a J-based stress intensity factor (K^+) was derived. The procedure is explained in the following sections.

Since it is not possible to evaluate Rice's J-integral [12] for an elliptical crack or for a semielliptical surface crack in a stress field with a gradient exactly, a solution derived by Shih and Hutchinson [13] was used for the determination of an equivalent J_{max}-value for the maximum load in the cycle (compare Fig. 10). This J_{max}-value is transformed into the newly defined J-based stress intensity factor $K^+_{max} = \sqrt{E \cdot J_{max}}$. For the unloading part of the cycle from σ_o = 392 MN·m^{-2} and ε_o = 1.0 % to σ_u = -8 MN·m^{-2} and ε_u = 0.4 % the J-integral definition by Rice cannot be used. In order to overcome this limitation, it was assumed that the J-integral calculation remains further applicable provided that for the stress-strain curve in the J-integral calculation not the basic material stress-strain law is used (which was also previously applied for the determination of the J_{max}-value) but the stress-strain curve of the material for an unloading condition after the maximum load was reached. This leads to a corresponding ΔK^+-value and, with $K^+_{min} = K^+_{max} - \Delta K^+$, to a K^+_{min}-value.

In the present case the stress-strain behaviour during unloading remained predominantly elastic. That means that ΔK^+ could be approximately evaluated on the basis of LEFM calculations. Because of the plasticity during the uploading in the present investigation the J-based ratio K^+_{min}/K^+_{max} had to be used instead of the conventional stress ratio ($R = \sigma_{min}/\sigma_{max}$). This ratio was then formally introduced into an Elber equation [14], which takes into account the crack closure influence. Fig. 10 shows that the value of the J-based ratio K^+_{min}/K^+_{max} was quite similar to the strain ratio $\varepsilon_u/\varepsilon_o$ which was applied in the tests. From that it was concluded that the strain ratio can be seen as a useful parameter to account for plasticity effects in combination with linear da/dN ΔK-calculations. This result is important for engineering considerations.

In Fig. 11 the constant amplitude crack growth rate of the individual microcracks is plotted versus the length of the surface cracks for the specimen with the most severe notch (K_t = 3.3). The squared symbols represent the test results, and the dashed line is an average curve through the experimental results. It can be seen that a crack growth calculation based on the stress ratio σ_u/σ_o is unsatisfactory (because it does not allow for the plasticity effects). The dash-dotted line shows the calculation result if the strain ratio $R_\varepsilon = \varepsilon_u/\varepsilon_o$ is used as it was suggested before. The test results are quite well in their trend except for very short crack lengths, where a slight tendency to underestimate the crack growth rate can be observed. If the scatter of the test results is not specially considered, a "short crack"-effect as it is reported in the literature (e.g. [3]) seems to be present as the crack length approaches microstructural sizes (grain size, inclusions etc.)

At large crack lengths the crack growth prediction deviates from the actual test results again. This may be attributed to the fact that large cracks have been formed due to the coalescence of several smaller cracks. The semielliptical surface cracks which have been formed in this manner exhibit an aspect ratio which is smaller than for the final crack lateron. As long as the final aspect ratio of the crack ellipse is not yet reached the crack growth at the notch surface is decreased.

Under variable amplitude loading conditions a behaviour of the microcracks was observed which was quite similar to that of large cracks. These investigation results are extensively discussed in [8].

CONCLUSIONS

- At the investigated 2024-T3 alloy crack initiation occurred at the Fe- and Si-containing intermetallic inclusions.
- A comparison of the fatigue behaviour of notched and of unnotched specimens with a same strain history at the unnotched specimen and at the notch root of a notched specimen showed that the equivalence between both situations decayed the more the loading level approached the endurance limit and the larger the crack lengths were defined for the end of the crack initiation stage.
- Fracture mechanics based analyses of the small crack behavior led to satisfactory predictions, if the influence of the stress gradient, of the crack geometry (shape), and of the plasticity was adequately taken into account.

ACKNOWLEDGEMENTS

The financial support of the DFG (Deutsche Forschungsgemeinschaft) is gratefully acknowledged. Also thanks are due to Herren H.J. Strunck and K.H. Trautmann for their experimental work and support.

SYMBOLS

a	= crack depth, crack length (µm)
c	= half the length of a surface crack (µm)
da/dN	= crack growth rate (mm/cycle)
dc/dN	= crack growth rate of surface cracks (mm/cycle)
K_c	= fracture toughness (MN·m$^{-3/2}$)
K_t	= elastic stress concentration factor
K_{CC}	= stress intensity factor for an embedded circular crack (MN·m$^{-3/2}$)
K_{NCC}	= stress intensity factor for an embedded circular crack within a stress gradient (MN·m$^{-3/2}$)
K_{EC}	= stress intensity factor for a semielliptical surface crack (MN·m$^{-3/2}$)

K_{NEC} = stress intensity factor for a semielliptical surface crack within a stress gradient ($MN \cdot m^{-3/2}$)
K^+ = equivalent stress intensity factor for plasticity ($N \cdot mm^{-3/2}$)
l = length of surface cracks (μm)
N = number of cycles
N_f = number of cycles to fracture
N_i = number of cycles to initiation
R = stress ratio
R = strain ratio
ε = local strain (%)
ε_F = (true) fracture strain
σ = stress ($MN \cdot m^{-2}$)
σ_y = yield stress ($MN \cdot m^{-2}$)
$\Sigma l_{i,net}$ = sum of the length of those microcracks leading to final failure (μm)

REFERENCES

1. Foth,J.,Nowack,H.,and Lütjering,G., Proc.4th Eur. Conf. on Fract., Leoben/Austria,(1982).

2. Foth,J.,"Einfluß von einstufigen und nicht-einstufigen Schwingbelastungen auf Rißbildung und Mikrorißausbreitung in Al 2024-T3",Dissertation, TU Hamburg-Harburg,(1983).

3. Miller,K.J.,Fat.Eng.Mats.Structs.,5(1982)No.3,223.

4. Nowack,H.,Hanschmann,D.,Foth,J.,Lütjering,G.,and Jacoby,G.,ASTM-STP 770,Am.Soc.Test.Mats.,(1982),269.

5. Hanschmann,D.,"Ein Beitrag zur rechnerischen Anrißlebensdauervorhersage schwingebanspruchter Kraftfahrzeugbauteile aus Aluminiumwerkstoffen",Dissertation, RWTH Aachen,(1981).

6. Crews,J.H.,and Hardrath,H.F.,Exp.Mech.,23(1966),313.

7. Lütjering,G.,and Gysler,A., Proc. 1st Int.Symp.Aluminum, Puerto Madryn, Argentina,(1978), ASM-publishing.

8. Foth,J.,Marissen,R.,Nowack,H.,and Lütjering,G., Proc.14th ICAS Congr., Toulouse/France,(1984), to be published.

9. Tada,H.,Paris,P.C.,and Irwin,G.R.,"The Stress Analysis of Cracks Handbook",Del Research Corp., St.Louis/USA.

10. Ott,W.,Proc. Werkstoff-Kolloquium DFVLR,Köln/Germany,(1982).

11. Newman,J.C.,and Raju,ASTM-STP 687,Am.Soc.Test.Mats.,(1979),16.

12. Rice,J.R.,"Fracture-An Advanced Treatise, Mathematical Fundamentals", Vol.2,Acad.Press, New York,(1968),191.

13. Shih,C.F.,and Hutchinson,J.W.,Journ.Eng.Mats.Techn.,(1976),289.

14. Elber,W.,ASTM-STP 486,Am.Soc.Test.Mats.,(1971),230.

FIGURES

	σ_y	NUCLEATION ϵ_F	NUCLEATION N_F	PROPAGATION K_C	PROPAGATION da/dN
UNDERAGED (coherent particles)	+	-	-	-	+
OVERAGED (semicoh. particles)	-	+	+	+	-
PFZ	o	-	-	-	-
DECREASING GRAIN SIZE	o+	+	+	+	-
INCLUSIONS (Fe, Si)	o	-	-	-	-
INCLUSIONS (Cr, Mn)	o	+	+	-	-
COLD DEFORMATION	+	-	+	o-	-

Figure 1: Qualitative evaluation of the influence of microstructural parameters on the crack nucleation and crack propagation behaviour under static and cyclic loading and on yield stress.

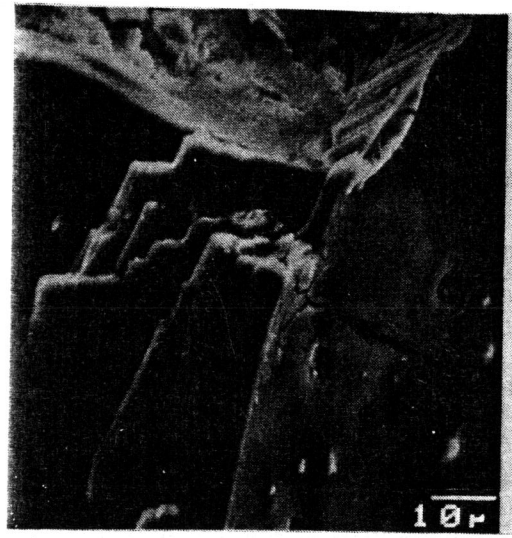

Figure 2: Fracture surface and notch root(SEM). Arrow indicates broken inclusion visible at the notch root surface.

Figure 3: Initiation of several microcracks from an inclusion during fatigue loading.

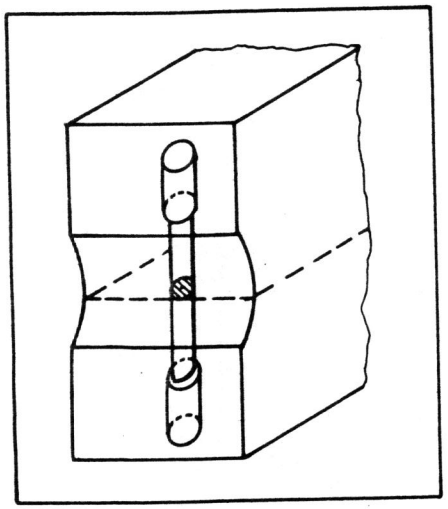

Figure 4: Companion specimen concept after [3].

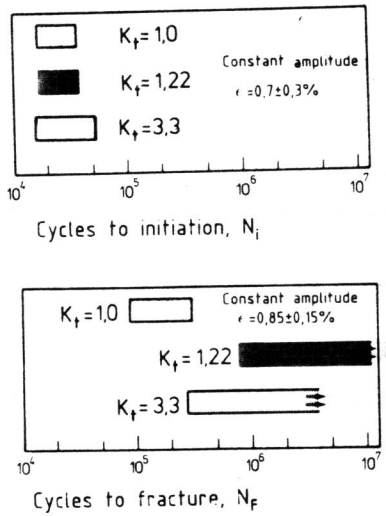

Figure 5: Crack initiation and fracture behaviour for different constant amplitude loadings.

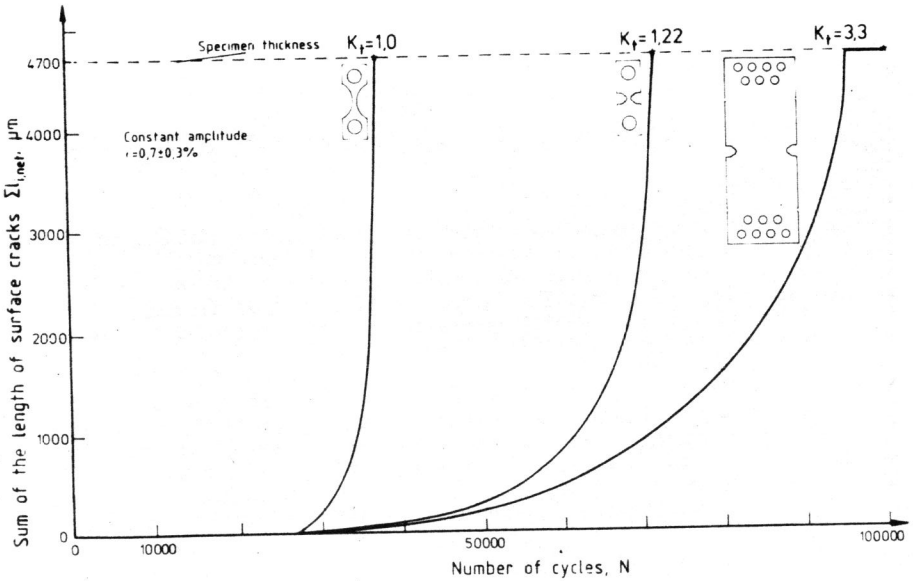

Figure 6: Microcrack initiation and propagation for the notched and for unnotched specimens.

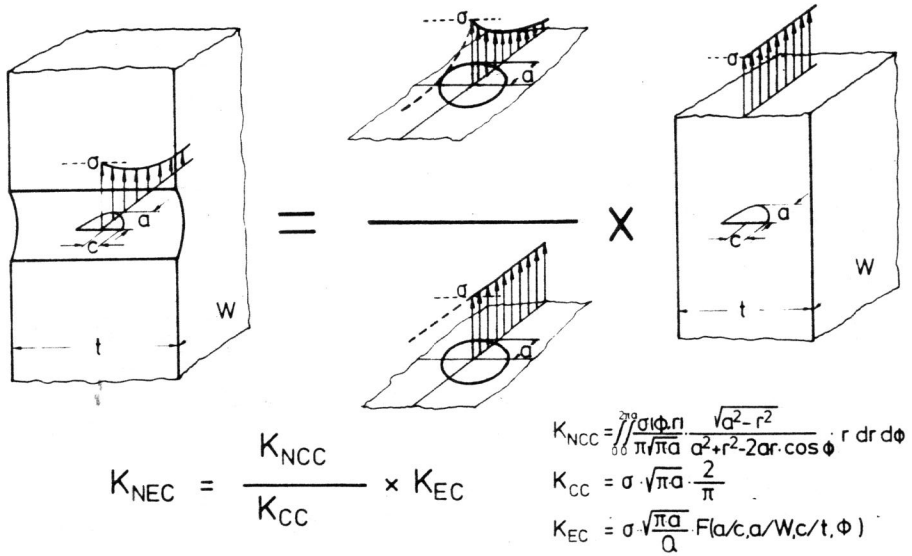

Figure 7: Superposition concept for the stress intensity factor for a semielliptical surface crack at a notch.

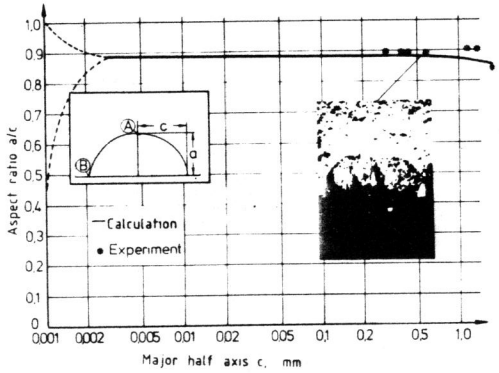

Figure 8: Crack shape as a function of the crack length: Calculation and experimental results

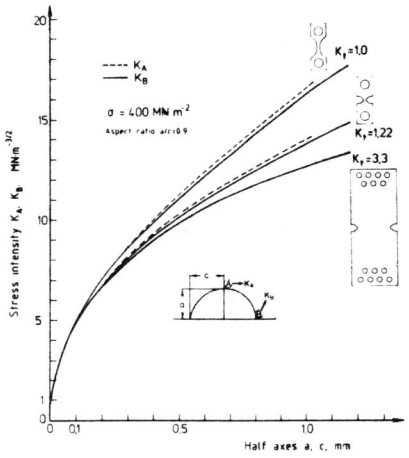

Figure 9: Stress intensity factor for semielliptical surface cracks for the notched specimens and for the unnotched specimen.

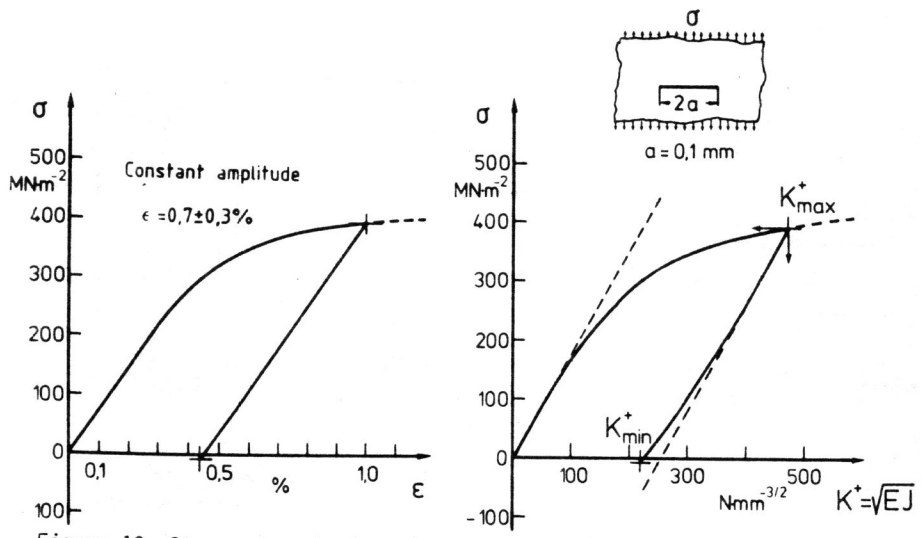

Figure 10: Stress vs. strain and stress vs. equivalent stress intensity factor K^+ as calculated on the basis of the elastic-plastic J-integral for constant amplitude loading.

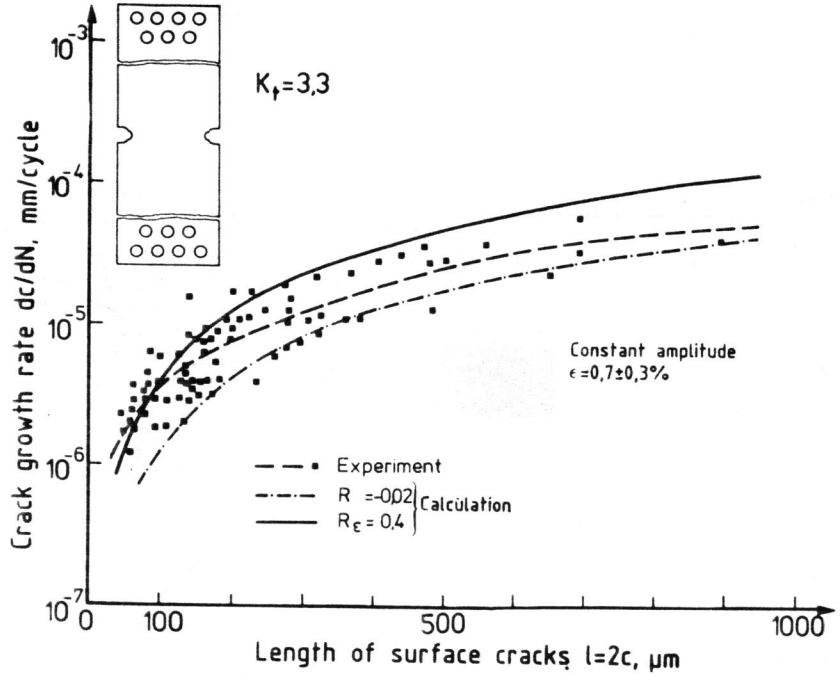

Figure 11: Microcrack growth behaviour of the K_t=3.3 specimen under constant amplitude loading.